Department of the Interior

U.S. Geological Survey

Differential Spectra for the 1979 El Centro and the 1984 Morgan Hill, California Earthquakes

by

G.N. Bycroft and P.N. Mork

U.S. Geological Survey[1]

Open-File Report 87-94

This report is preliminary and has not been reviewed for conformity with U.S. Geological Survey editorial standards and stratigraphic nomenclature.

[1]Menlo Park, California

1987

Differential Displacements and Spectra for the 1979 El Centro and the 1984 Morgan Hill Earthquakes

G. N. Bycroft and P. N. Mork

Abstract

Differential ground motion, under the base of a structure, imposes direct strain on the structure in addition to the strains caused by inertial loading. In order to assess the importance of these differential strains, differential arrays of digital accelerometers with pre-event memory were installed at El Centro and Hollister, California. These arrays produced useful data for the 1979 El Centro, the 1984 Morgan Hill, the 1981 Westmorland, and the 1986 Hollister earthquakes. This report gives differential displacements and spectra for the 1979 El Centro and the 1984 Morgan Hill earthquakes. In certain circumstances the differential strains are significant.

Introduction

Seismic design generally has assumed that all points on the ground move in unison with the free-field motion over a region that is larger than the foundation of the structure. This assumption is based on the notion that seismic waves are substantially propagated substantially in high-wave-velocity basement rock and transmitted vertically to the region of interest through lower velocity layers. However, surface waves propagating horizontally through surface layers may have wavelengths along the surface of approximately the dimensions of a large structure (Trifunac, 1972; Wong and Trifunac, 1974; Bycroft, 1980). Further, differential ground motion may be caused by local inhomogeneity. The foundation of the structure would then undergo differential motions that would cause additional strains to be superimposed on those

geneity. The foundation of the structure would then undergo differential motions that would cause additional strains to be superimposed on those due to inertial loading. Thus, for example, adjacent bridge piers would move relative to each other and cause stresses in the piers and the bridge decking. Structures built on spread footings, dams and pipelines would be similarly affected.

To study such motion, differential ground motions must be measured. Methods of utilizing this information in seismic design should be developed. Arrays of seismometers have been installed at El Centro and Hollister, California. These arrays are discussed in Bycroft (1982, 1983). Figure 1 shows the configuration of the Hollister array. The El Centro array runs north and south at distances of 0, 60, 180, 420, 700, and 1000 feet.

Differential Displacements

Differential spectra are defined as spectra combining both differential and inertial strains. In order to calculate differential spectra it is necessary to calculate differential displacements. The processing of accelerograms to give displacements has long been a problem due to the double integrations of base-line error, long-period noise, quantification errors, and problems related to the mechanics of film transportation. The original processing was directed towards digitized film records and was developed initially at the California Institute of Technology. Many changes have been made at the U.S. Geological Survey resulting in the present form known as AGRAM (Converse, 1984). This program has many options available depending on the judgement of the user for his particular application or data. The processing includes instrument corrections, base line corrections and high-pass filtering to eliminate long-period noise and quantification errors.

The program uses a Butterworth filter on the velocity running both ways to correct for phase. This, however, together with an inadequate base-line correction, leads to a finite initial velocity which, when integrated, leads to an initial rise or fall in the displacement, increasing with the long period cut-off of the high pass filter. Displacements themselves are of no interest because only the difference of displacements occurs in structural equations. Consequently, only differences of displacements are considered. This difference will eliminate those real long period seismic signals whose wavelengths are large compared to the spacing of the stations. The processing adopted was to find a system which, for a series of long period cut-offs would give reasonably similar differences with a minimum of rise or fall in the beginning of the calculated differences. This process, for the two earthquakes considered here, is discussed in Bycroft and Mork, 1986.

Differential Spectra

In order to examine the significance of a structure being subjected to differential strain loading, in addition to the inertial loading, a simple model which is affected by both these loadings was investigated. Figure 2 shows this structure as a simple one-span bridge type of structure with two vertical piers connected by a deck. Transverse horizontal ground motions are applied to this structure so that shear stresses are developed in the three components. The masses are lumped together where the deck joins the piers. The two masses are each equal to m, the stiffness of the piers is k_1 and the stiffness of the deck is k_2. Different horizontal displacements $y_1(t)$ and $y_2(t)$ are applied to the base of each pier. A response spectrum R was calculated. This response spectrum is defined as the ratio of the maximum strain in pier 1 when the displacement inputs are $y_1(t)$ and $y_2(t)$ to the

maximum strain in pier 1 when $y_1(t) = y_2(t)$. As these two displacements are nearly equal it matters little which one is used for the reference. $y_1(t)$ was used. This ratio R is then a suitable measure of the effect of the addition of differential strain to the inertial loading. It is readily shown that

$$R = \frac{A}{B} \tag{1}$$

where

$$A = \frac{\text{Max}}{2} \int_0^t C \, d\tau \tag{2}$$

where Max means the maximum value of the integral during the length of the input and where

$$C = \frac{e^{-\lambda\omega_1(t-\tau)}\{\ddot{y}_1(\tau)+\ddot{y}_2(\tau)\}\sin\omega_1(t-\tau)}{\omega_1} + e^{-\lambda\sqrt{\omega_1^2+2\omega_2^2}\,(t-\tau)}[\ddot{y}_1(\tau)-\ddot{y}_2(\tau)+2\omega_2^2\{y_1(\tau)-y_2(\tau)\}]\sin[\sqrt{\omega_1^2+2\omega_2^2}(t-\tau)] \Big/ \sqrt{\omega_1^2+2\omega_2^2} \tag{3}$$

$$B = \text{Max} \int_0^t \frac{e^{-\lambda\omega_1(t-\tau)}\ddot{y}_1(\tau)[\sin\omega_1(t-\tau)]\,d\tau}{\omega_1} \tag{4}$$

where

$$\omega_1 = \sqrt{\frac{k_1}{m}} \tag{5}$$

$$\omega_2 = \sqrt{\frac{k_2}{m}} \tag{6}$$

(7) λ = modal damping factor

These spectra are for a simple two degree of freedom structure and are

more relevant to situations where the two stations are closer. A multi-degree-of-freedom spectra is being developed that is more relevant to stations farther apart.

The differential spectra for the Hollister records of the 1984 Morgan Hill earthquake are shown in Figures 3, 4, 5, and 6 for station 3 minus station 1 for $\omega_1 = \omega_2$ and $\omega_2 = 10, 30, 50$ for transverse horizontal motion with no damping. It is seen that for low values for ω_1 and ω_2 the ratio R is around unity as would be expected. However, as the structure is stiffened the effect of the imposition of differential strain becomes apparent. For very stiff structures the effect of differential strains dominates over those caused by the inertial loading. The variations in the differential spectra are not only a function of structural frequencies and damping but also directly related to the frequency contents of $y_1(t)$ and $y_2(t)$. In the extreme case where the masses tend to zero thus making the natural frequencies tend to infinity the inertial loading tends to zero and the ratio R tends to infinity. Figures 7, 8 and 9 show the effect of damping on the ratio R between station 3 and 4 when $\omega_1 = \omega_2$. Damping has its main effect on the inertial terms and consequently damping increases the value of R. Figures 10, 11, and 12 show the spectra for station 4 minus 1 for different values of damping. It should be pointed out that some of these stations are relatively far apart for a realistic structure to be modelled in this simple way. The two closest station numbers 3 and 4 are somewhat more realistic.

Figures 13 to 24 show the differential spectra for the array's transverse component from the El Centro earthquake. The ratio R is generally smaller than those of the Hollister earthquake because the differential placements are relatively smaller.

Conclusions

For a stiff structure on separate foundations the stresses caused by differential ground motion are significant. The spectra shown only have a practical use for the stations closest together. Similar spectra should be calculated for multi-degree-of-freedom structures.

References

Bycroft, G.N., 1980, Soil foundation interaction and differential ground motions: Journal of Earthquake Engineering and Structural Dynamics, v. 8, no. 5, p. 397-404.

Bycroft, G.N., 1982, El Centro differential ground motion array: U.S. Geological Survey Professional Paper 1254, p. 351-356.

Bycroft, G.N., 1983, Differential ground motion array at Hollister Municipal Airport, California: U.S. Geological Survey Open-File Report No. 83-327.

Bycroft, G.N., and Mork, P.N., 1986, Differential ground motions and their spectra: Journal of Engineering Mechanics, A.S.C.E., (in press).

Converse, A.M., 1984, AGRAM: A series of computer programs for processing digitized strong-motion accelerograms, version 2.0: U.S. Geological Survey Open File Report 84-525, 118 p.

Trifunac, M.D., 1972, Interaction of a shear wall with the soil for incident plane SH waves: Seismological Society of America Bulletin, v. 62, no. 1, p. 63-83.

Wong, H.L., and Trifunac, M.D., 1974, Interaction of a shear wall with the soil for incident plane SH waves: Elliptical rigid foundation: Seismological Society of America Bulletin, v. 64, no. 6., p. 1825-1842.

Figure Captions

Fig. 1 Configuration of Hollister Differential Array.

Fig. 2 Model for differential spectra.

Fig. 3 Hollister 1984, spectral ratio R as a function of ω_1, station 3 minus station 1, $\omega_1 = \omega_2$, $\lambda = 0$.

Fig. 4 Hollister 1984, spectral ratio R as a function of ω_1, station 3 minus station 1 $\omega_2 = 10$, $\lambda = 0$.

Fig. 5 Hollister 1984, spectral ratio R as a function of ω_1, station 3 minus station 1 $\omega_2 = 30$, $\lambda = 0$.

Fig. 6 Hollister 1984, spectral ratio R as a function of ω_1, station 3 minus station 1, $\omega_1 = 50$, $\lambda = 0$.

Fig. 7 Hollister 1984, spectral ratio R as a function of ω_1, station 4 minus station 3, $\omega_2 = \omega_1$, $\lambda = 0$.

Fig. 8 Hollister 1984, spectral ratio R as a function of ω_1, station 4 minus station 3, $\omega_1 = \omega_2$, $\lambda = 0.1$.

Fig. 9 Hollister 1984, spectral ratio R as a function of ω_1, station 4 minus station 3, $\omega_1 = \omega_2$, $\lambda = 0.2$.

Fig. 10 Hollister 1984, spectral ratio R as a function of ω_1, station 4 minus station 1, $\omega_1 = \omega_2$, $\lambda = 0$.

Fig. 11 Hollister 1984, spectral ratio R as a function of ω_1, station 4 minus station 1, $\omega_1 = \omega_2$, $\lambda = 0.1$.

Fig. 12 Hollister 1984, spectral ratio R as a function of ω_1, station 4 minus station 1, $\omega_1 = \omega_2$, $\lambda = 0.2$.

Fig. 13 El Centro, 1979, spectral ratio R as a function of ω_1, station 2 minus station 1, $\omega_2 = 10$, $\lambda = 0$.

Fig. 14 El Centro, 1979, spectral ratio R as a function of ω_1, station 2 minus station 1, $\omega_1 = \omega_2$, $\lambda = 0$.

Fig. 15 El Centro, 1979, spectral ratio R as a function of ω_1, station 2 minus station 1, $\omega_1 = \omega_2$, $\lambda = 0.1$.

Fig. 16 El Centro, 1979, spectral ratio R as a function of ω_1, station 2 minus station 1, $\omega_1 = \omega_2$, $\lambda = 0.2$.

Fig. 17 El Centro, 1979, spectral ratio R as a function of ω_1, station 3 minus station 1, $\omega_2 = 10$, $\lambda = 0$.

Fig. 18 El Centro, 1979, spectral ratio R as a function of ω_1, station 3 minus station 1, $\omega_1 = \omega_2$, $\lambda = 0$.

Figure Captions (continued)

Fig. 19 El Centro, 1979, spectral ratio R as a function of ω_1, station 3 minus station 1, $\omega_1 = \omega_2$, $\lambda = 0.1$.

Fig. 20 El Centro, 1979, spectral ratio R as a function of ω_1, station 3 minus station 1, $\omega_1 = \omega_2$, $\lambda = 0.2$.

Fig. 21 El Centro, 1979, spectral ratio R as a function of ω_1, station 3 minus station 2, $\omega_2 = 10$, $\lambda = 0$.

Fig. 22 El Centro, 1979, spectral ratio R as a function of ω_1, station 3 minus station 2, $\omega_1 = \omega_2$, $\lambda = 0$.

Fig. 23 El Centro, 1979, spectral ratio R as a function of ω_1, station 3 minus station 2, $\omega_1 = \omega_2$, $\lambda = 0.1$.

Fig. 24 El Centro, 1979, spectral ratio R as a function of ω_1, station 3 minus station 2, $\omega_1 = \omega_2$, $\lambda = 0.2$.

HOLLISTER DIFFERENTIAL DIGITAL ARRAY

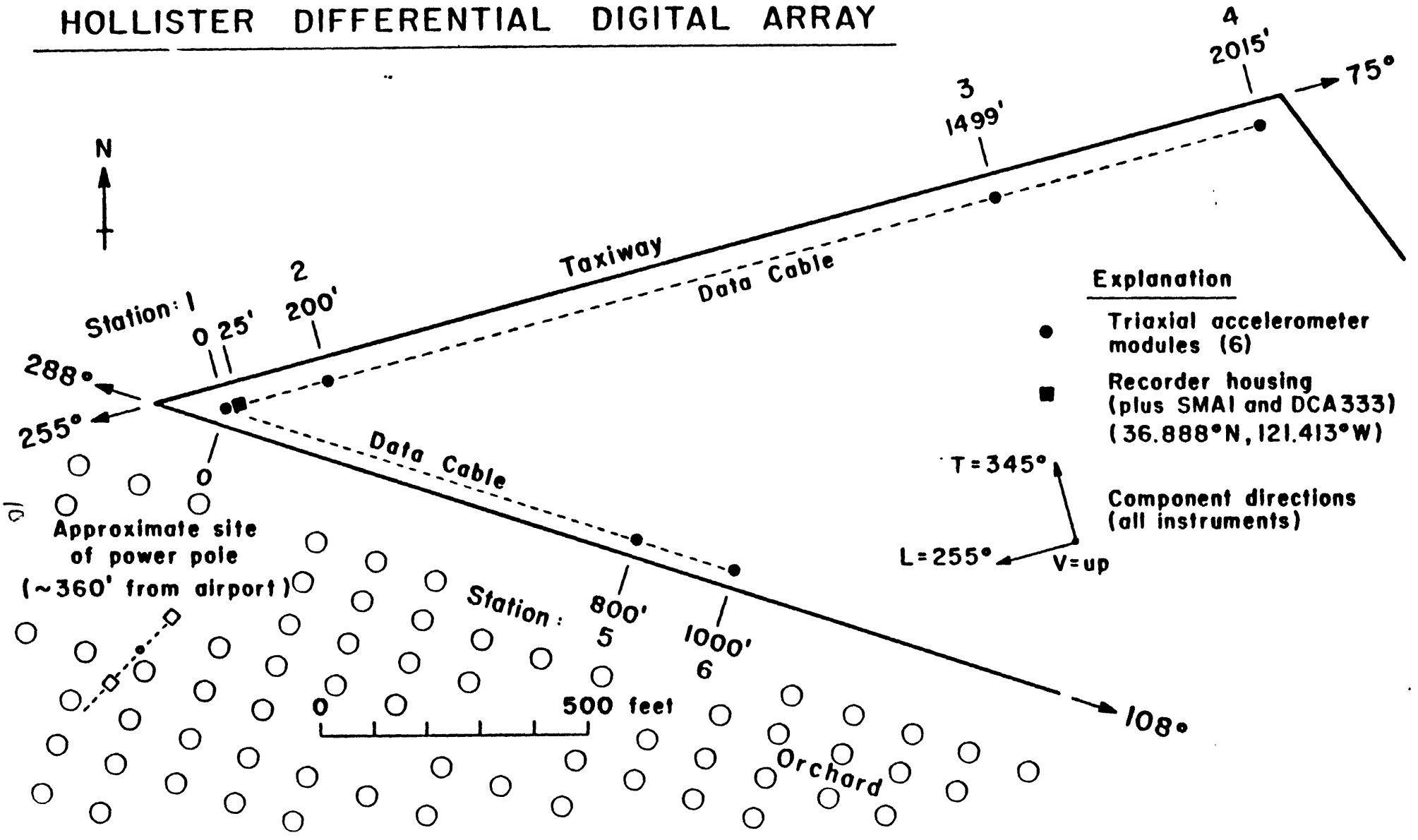

FIGURE 1

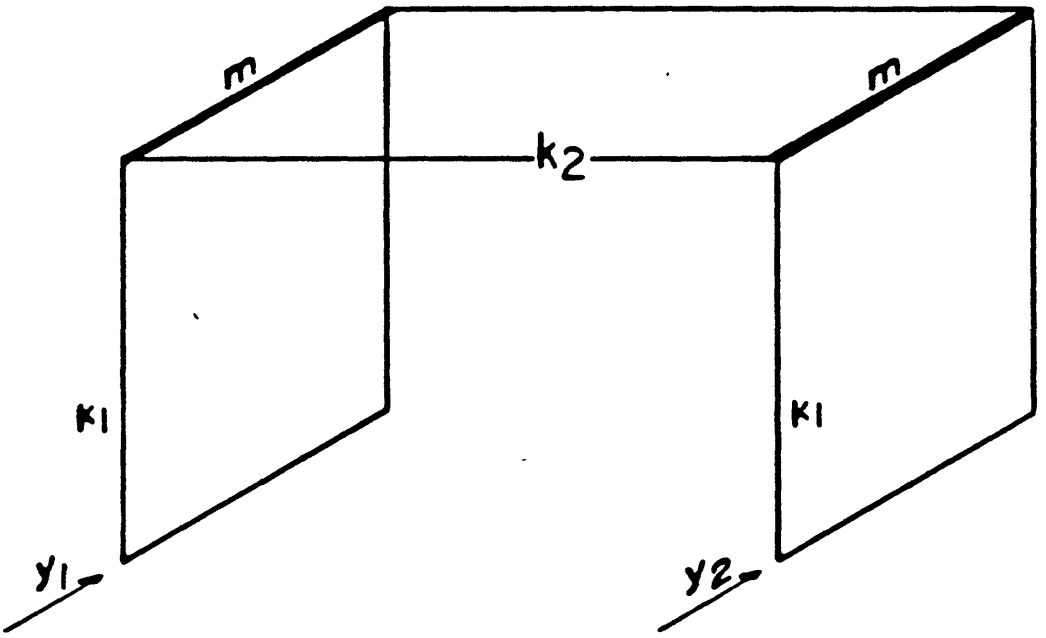

Fig 2

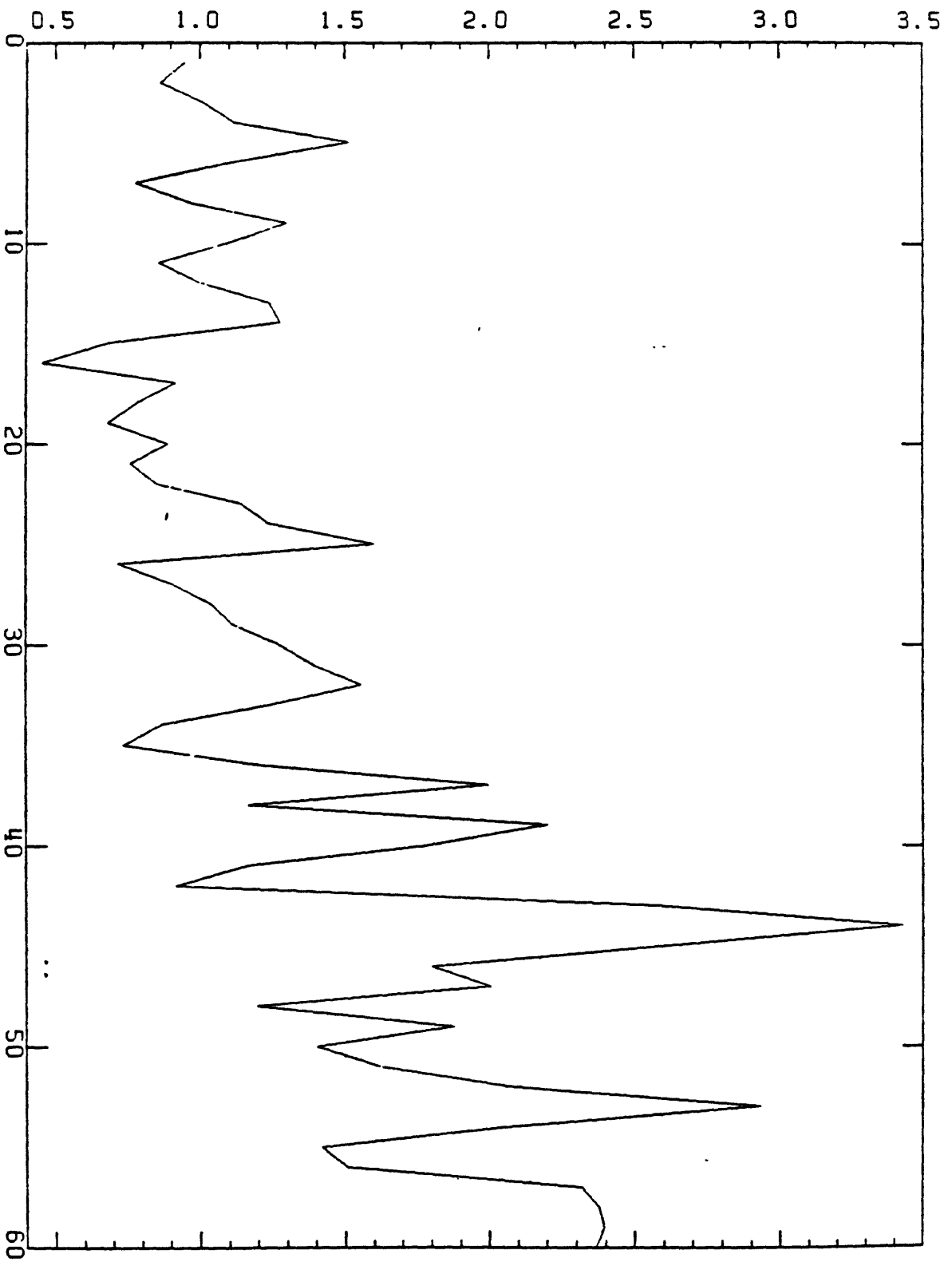
RATIO
0.5
1.0
1.5
2.0
2.5
3.0
3.5
0
10
20
30
40
50
60
OMEGA 1
DIFF3-DIFF1, OMEGA 2 = OMEGA 1 DAMPING = 0.0, LENGTH = 25. SEC, CHANNEL 03

Fig 3.

DIFF3-DIFF1, OMEGA 2 = 10 DAMPING = 0.0, LENGTH = 25. SEC, CHANNEL 03
RATIO
2.5
2.0
1.5
1.0
0
10
20
30
40
50
60
OMEGA 1

Fig 4

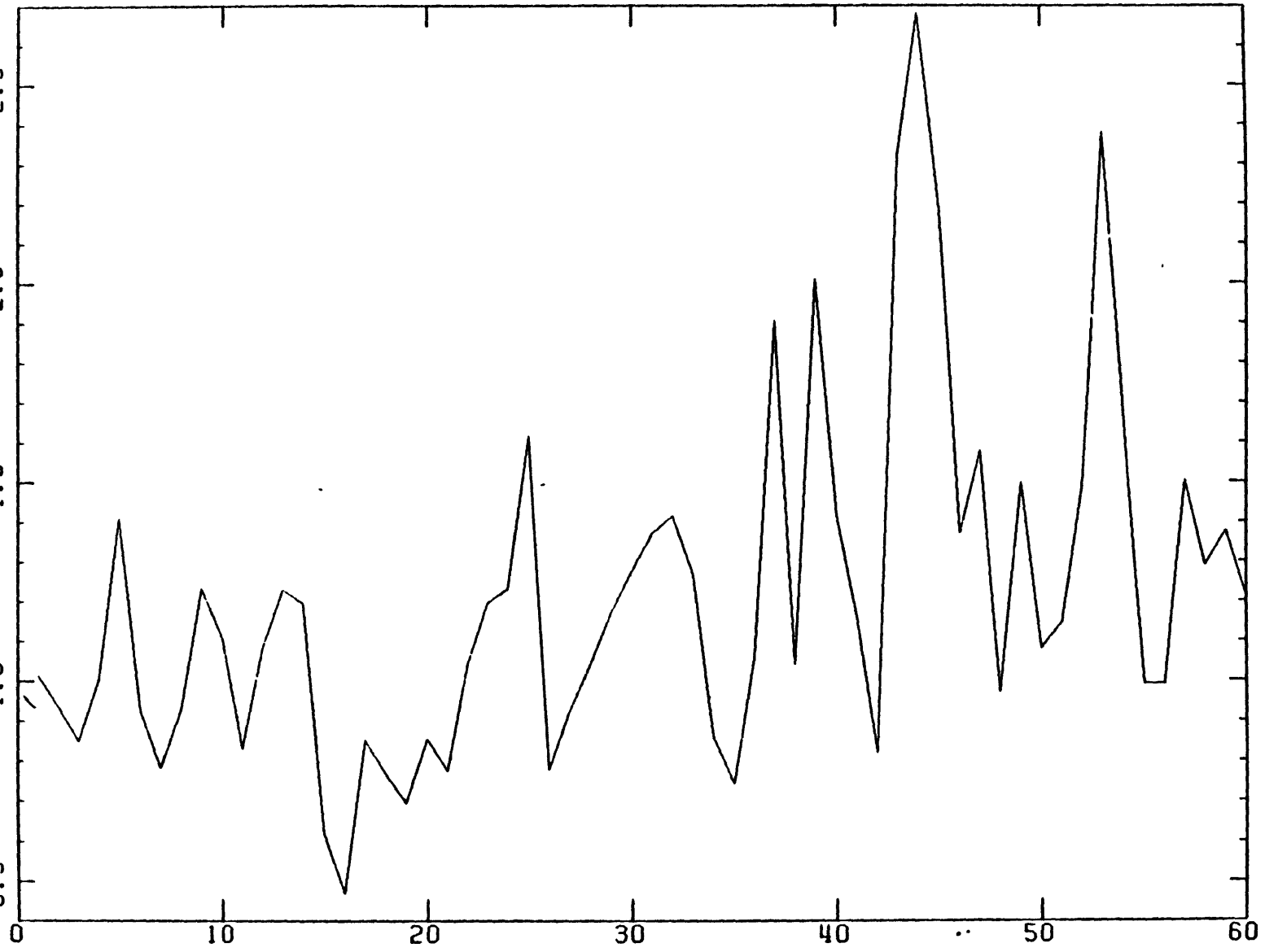
DIFF3-DIFF1, OMEGA 2 = 30 DAMPING = 0.0, LENGTH = 25. SEC, CHANNEL 03
RATIO
0.5
1.0
1.5
2.0
2.5
0
10
20
30
40
50
60
OMEGA 1

Fig 5

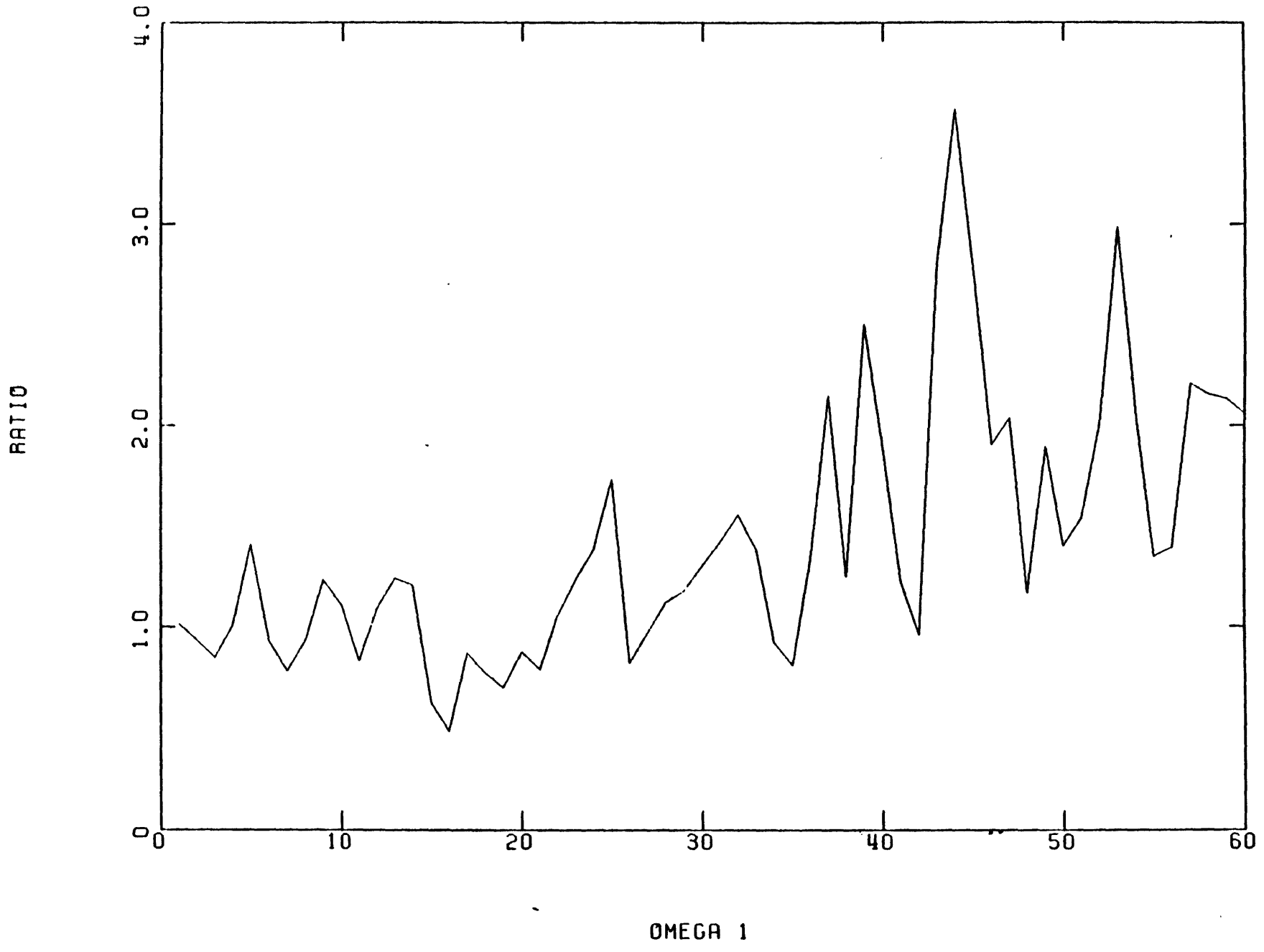
DIFF3-DIFF1, OMEGA 2 = 50 DAMPING = 0.0, LENGTH = 25. SEC, CHANNEL 03
RATIO
OMEGA 1
0
1.0
2.0
3.0
4.0
0
10
20
30
40
50
60

Fig 6

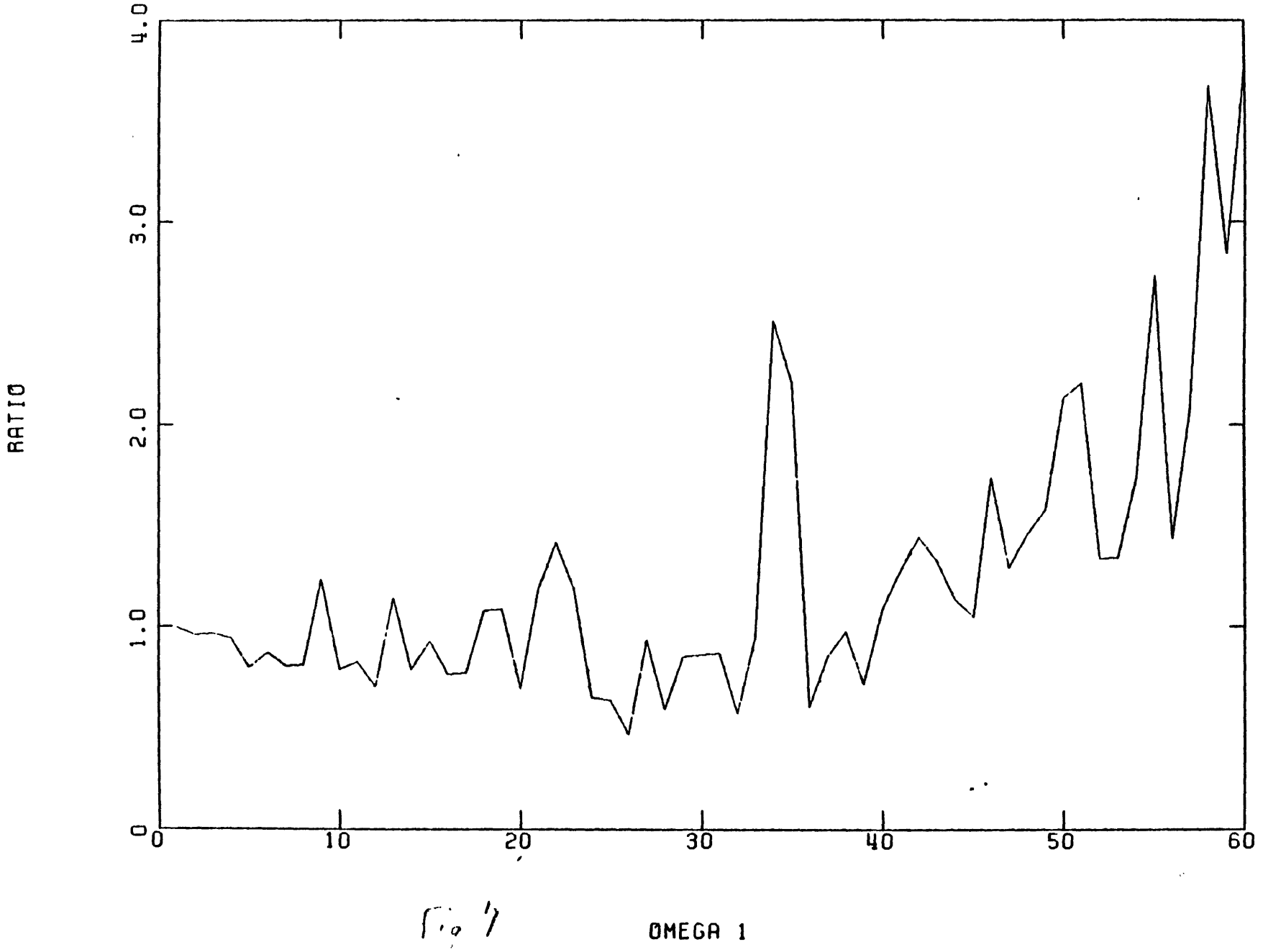
DIFF4-DIFF3, OMEGA 2 = OMEGA 1 DAMPING = 0.0, LENGTH = 40. SEC, CHANNEL 03
RATIO
0
1.0
2.0
3.0
4.0
0
10
20
30
40
50
60
OMEGA 1

Fig 7

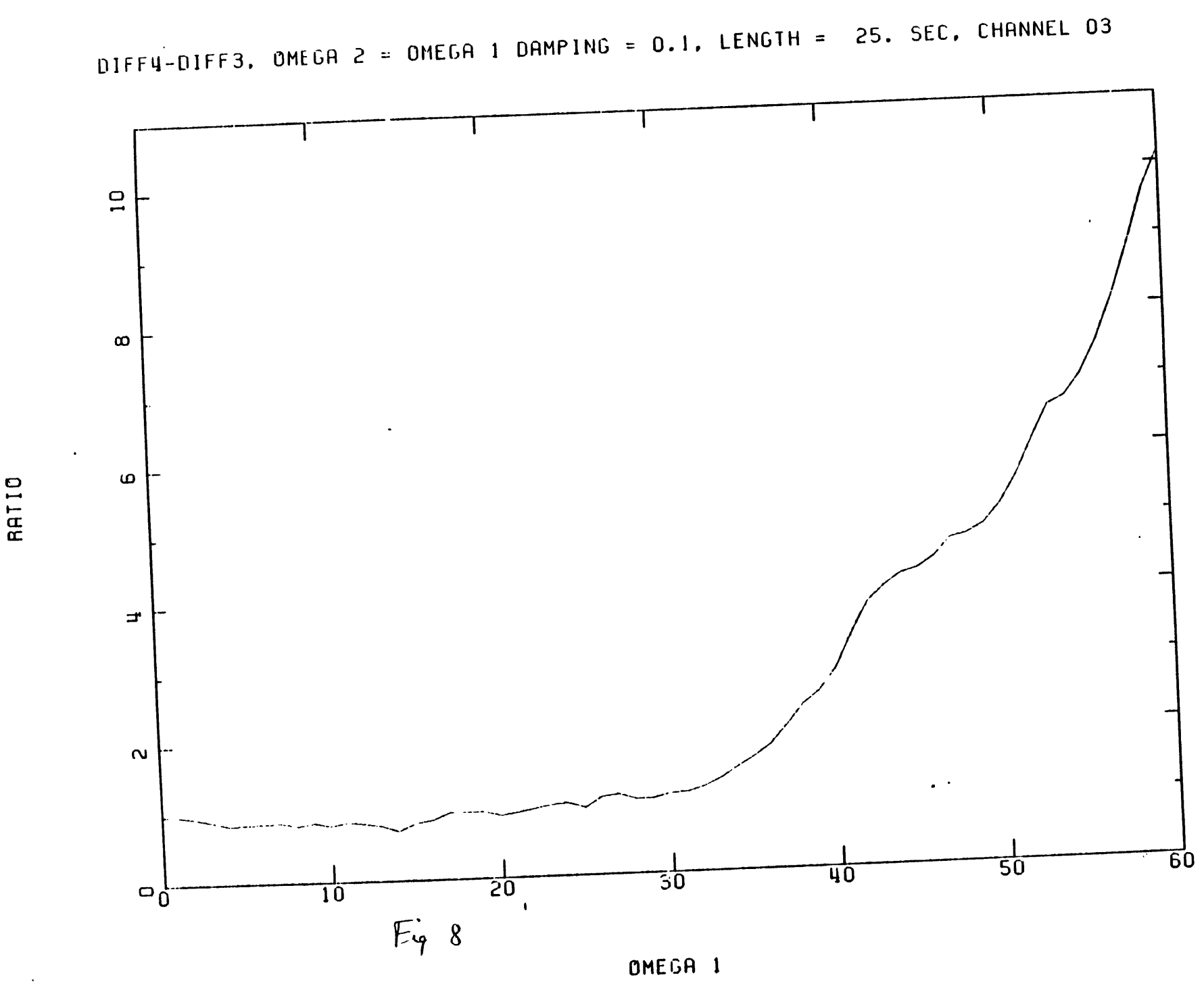
DIFF4-DIFF3, OMEGA 2 = OMEGA 1 DAMPING = 0.1, LENGTH = 25. SEC, CHANNEL 03
RATIO
0
2
4
6
8
10
0
10
20
30
40
50
60
OMEGA 1

Fig 8

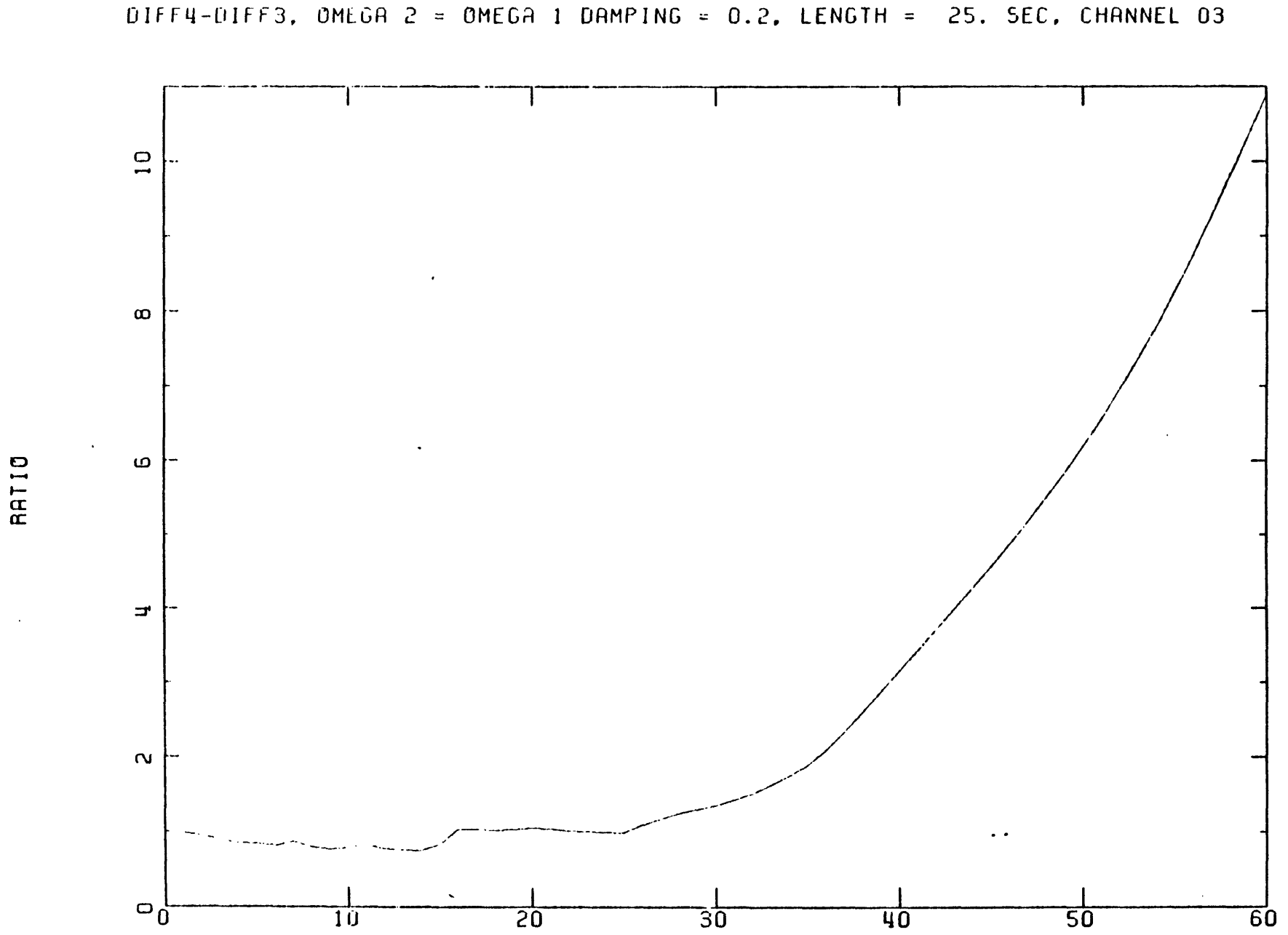
DIFF4-DIFF3, OMEGA 2 = OMEGA 1 DAMPING = 0.2, LENGTH = 25. SEC, CHANNEL 03
RATIO
0
2
4
6
8
10
0
10
20
30
40
50
60
OMEGA 1

Fig 9

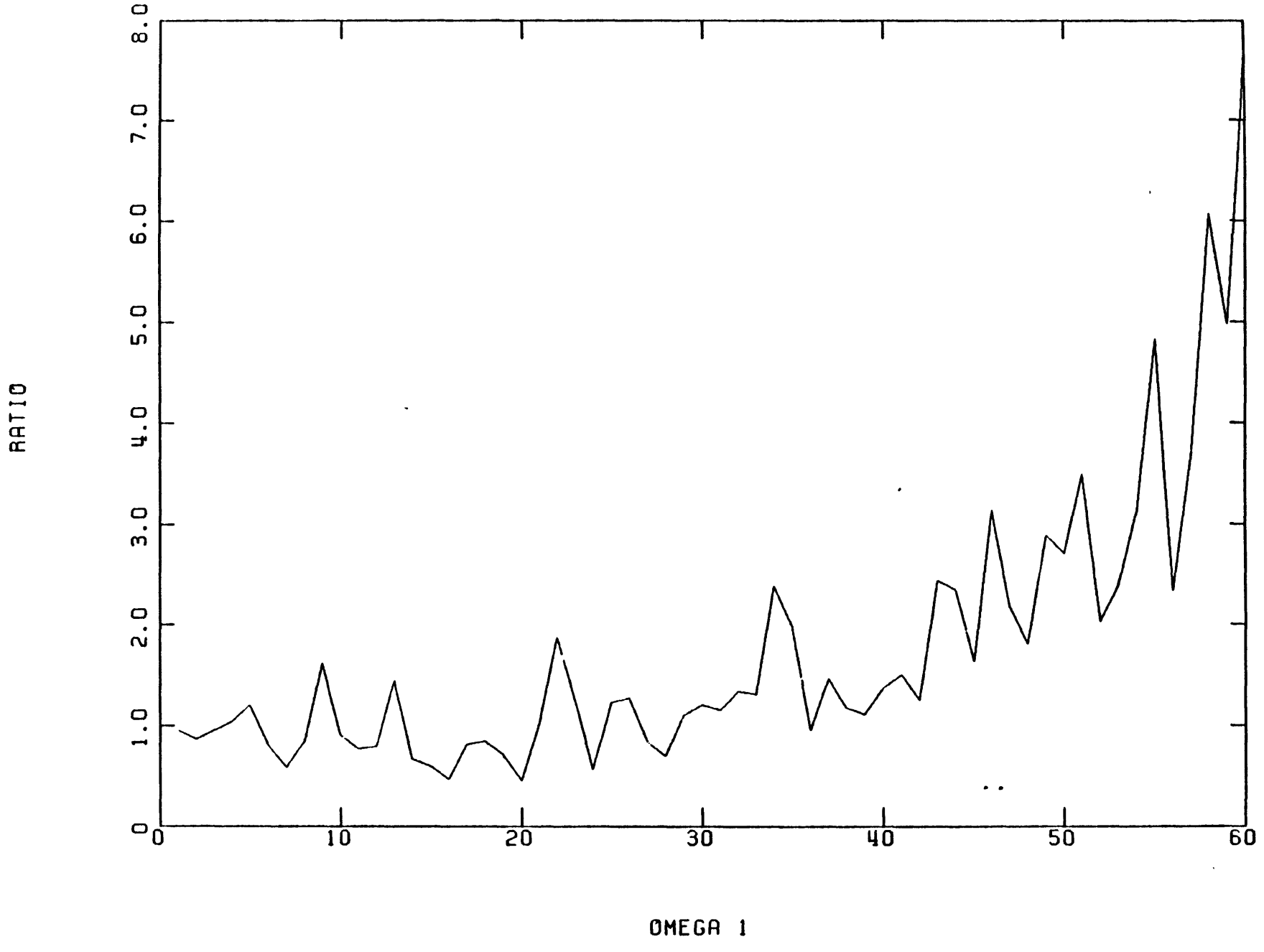
DIFF4-DIFF1, OMEGA 2 = OMEGA 1 DAMPING = 0.0, LENGTH = 25. SEC, CHANNEL 03
RATIO
0
1.0
2.0
3.0
4.0
5.0
6.0
7.0
8.0
0
10
20
30
40
50
60
OMEGA 1

Fig 10

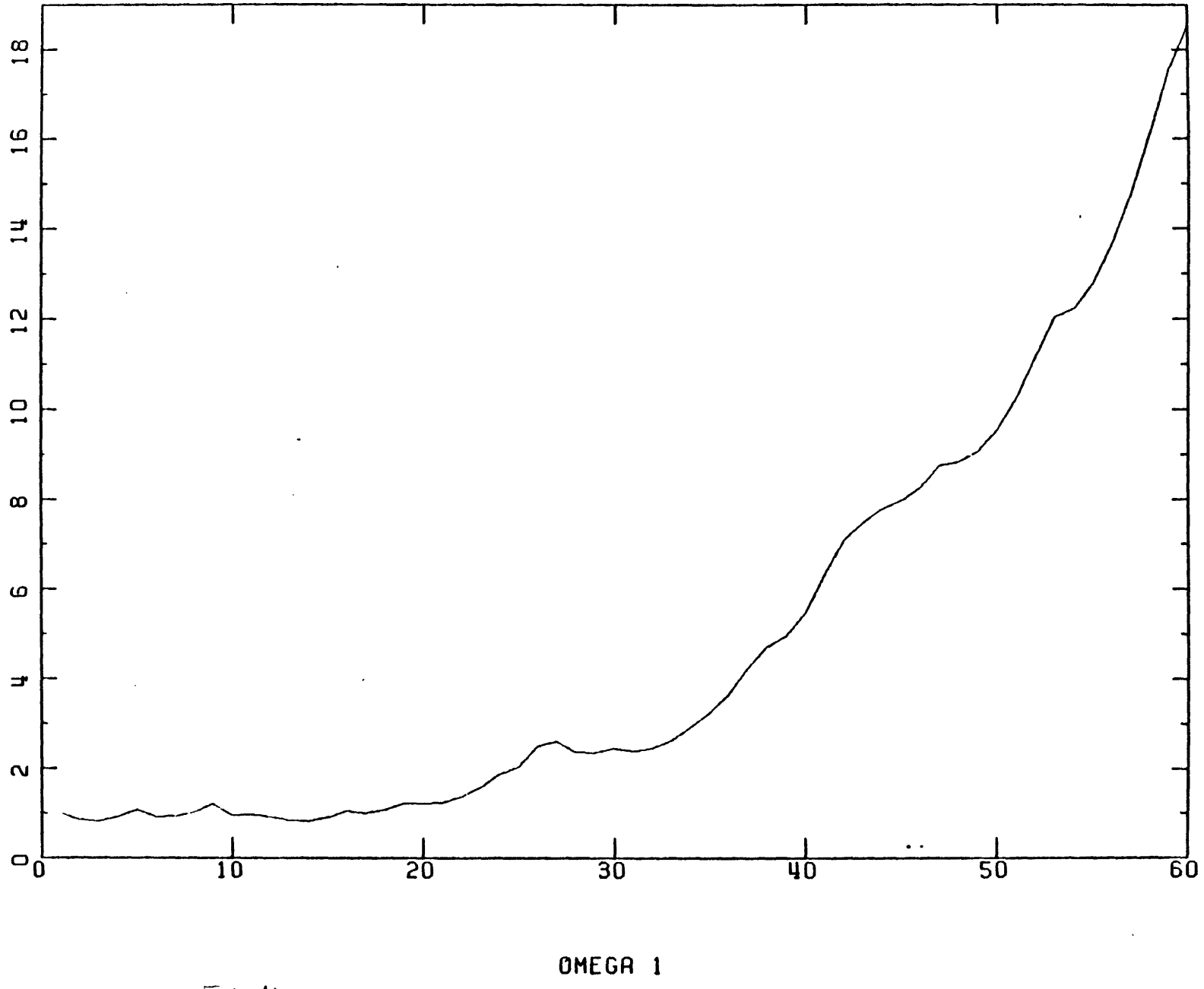
DIFF4-DIFF1, OMEGA 2 = OMEGA 1 DAMPING = 0.1, LENGTH = 25. SEC, CHANNEL 03
RATIO
0
2
4
6
8
10
12
14
16
18
0
10
20
30
40
50
60
OMEGA 1

Fig 11

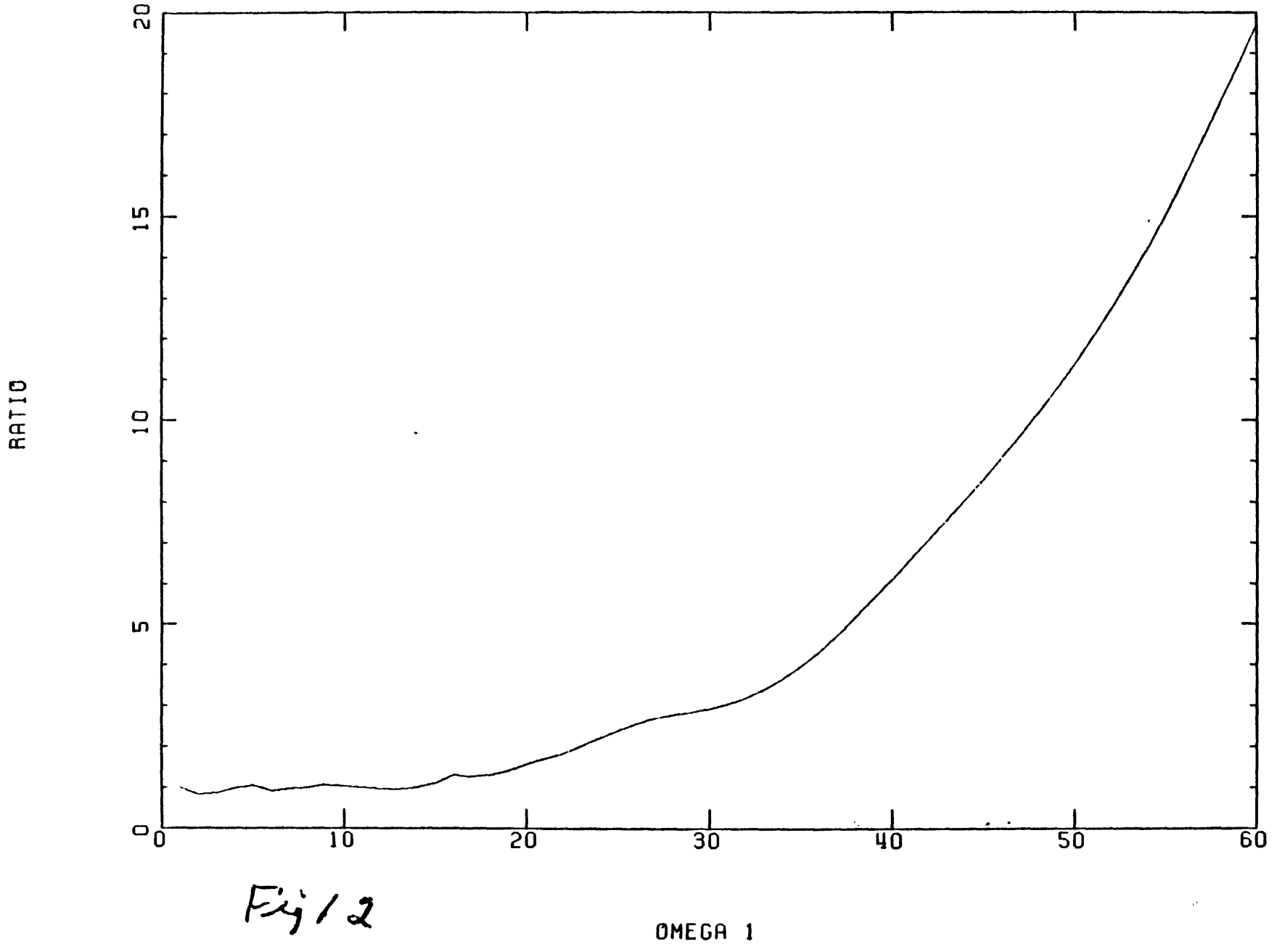
DIFF4-DIFF1, OMEGA 2 = OMEGA 1 DAMPING = 0.2, LENGTH = 25. SEC, CHANNEL 03
RATIO
0
5
10
15
20
0
10
20
30
40
50
60
OMEGA 1

Fig 12

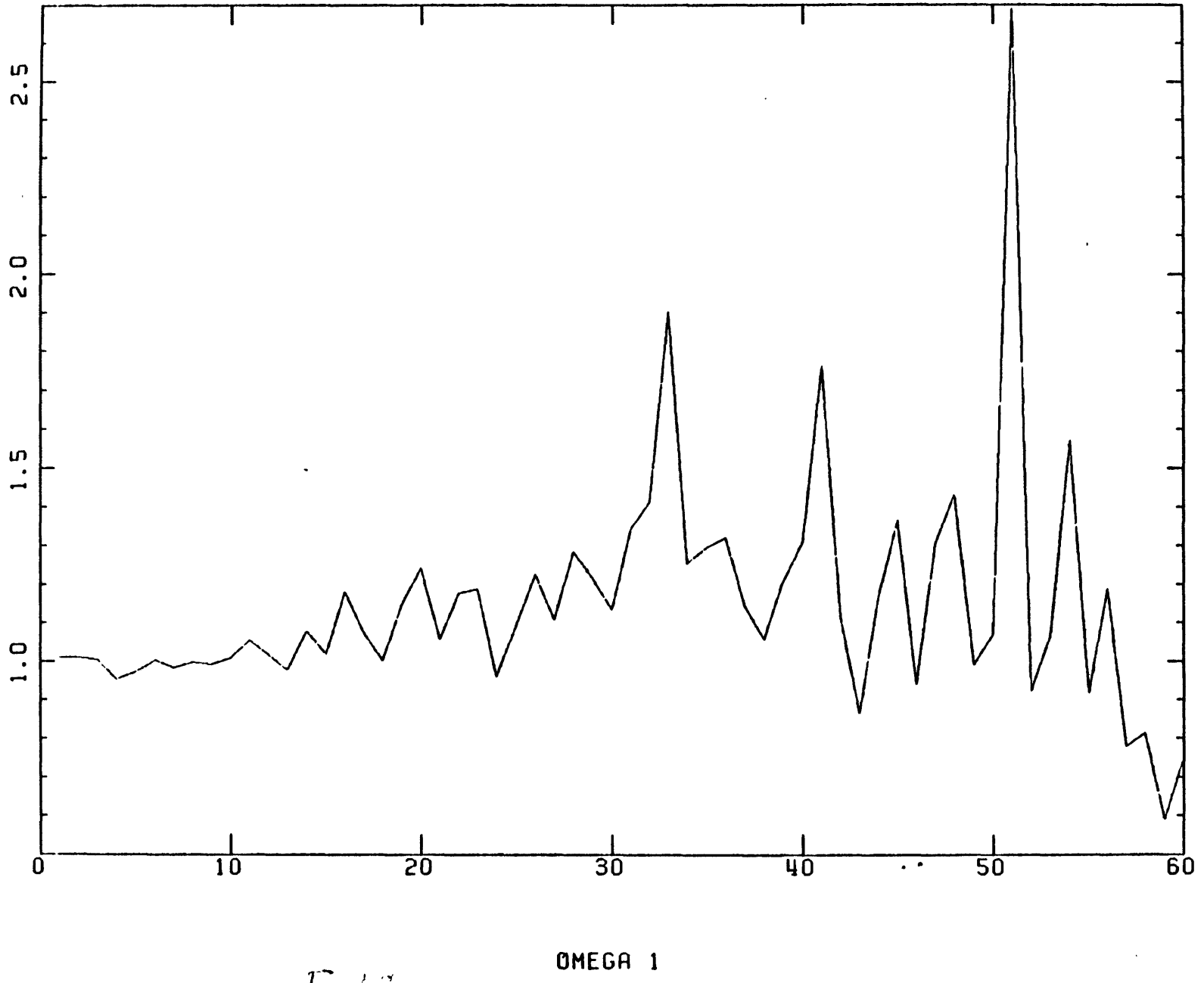
IVDA2-IVDA1, OMEGA 2 = 10.0, CHANNEL 02
RATIO
2.5
2.0
1.5
1.0
0
10
20
30
40
50
60
OMEGA 1

Fig 13

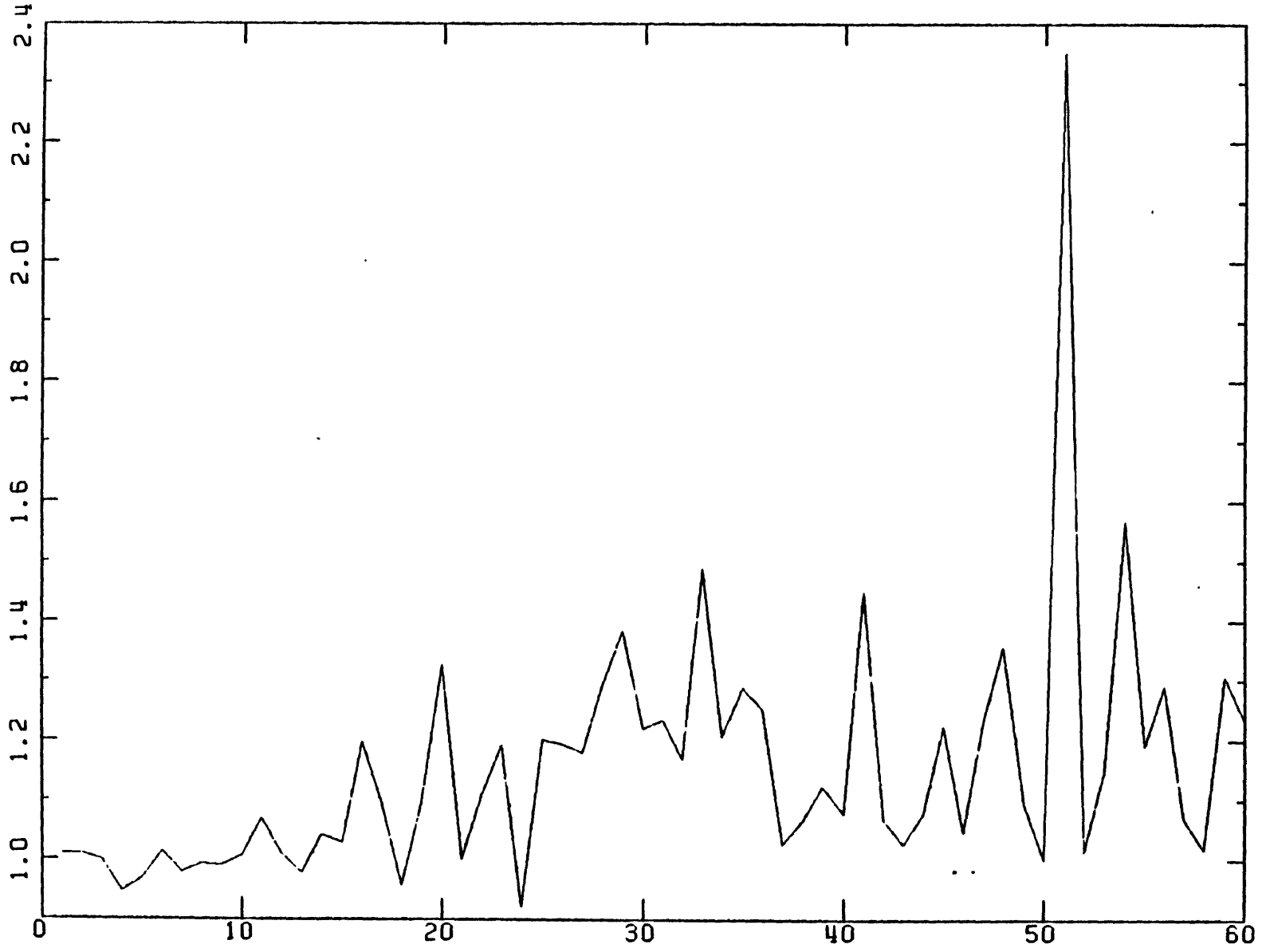
IVDA2-IVDA1, OMEGA 2 = OMEGA 1, CHANNEL 02
RATIO
1.0
1.2
1.4
1.6
1.8
2.0
2.2
2.4
0
10
20
30
40
50
60
OMEGA 1

Fig 14

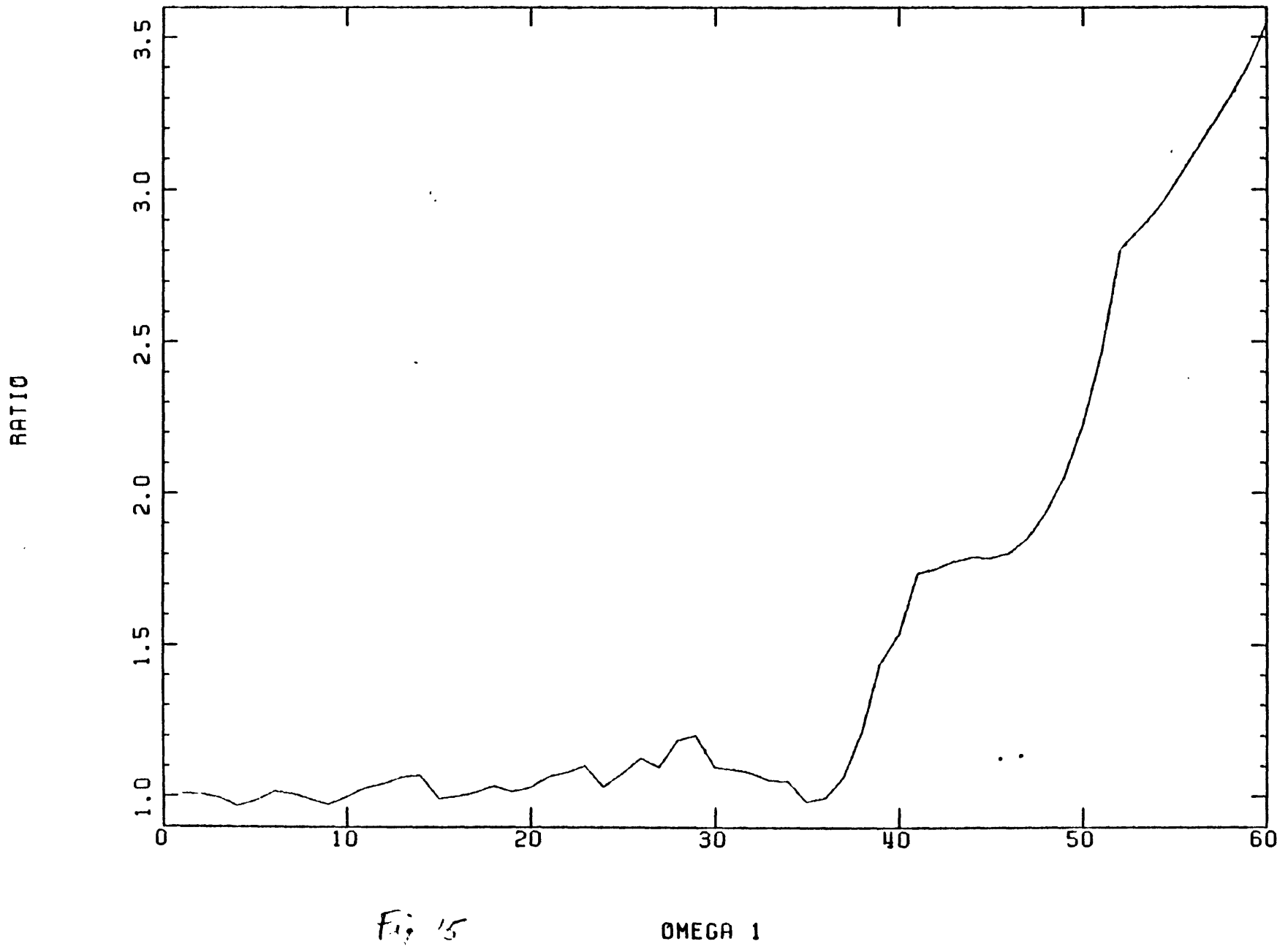
IVDA2-IVDA1, OMEGA 2 = OMEGA 1 DAMPING = .1, CHANNEL 02
RATIO
1.0
1.5
2.0
2.5
3.0
3.5
0
10
20
30
40
50
60
OMEGA 1

h2

Fig 15

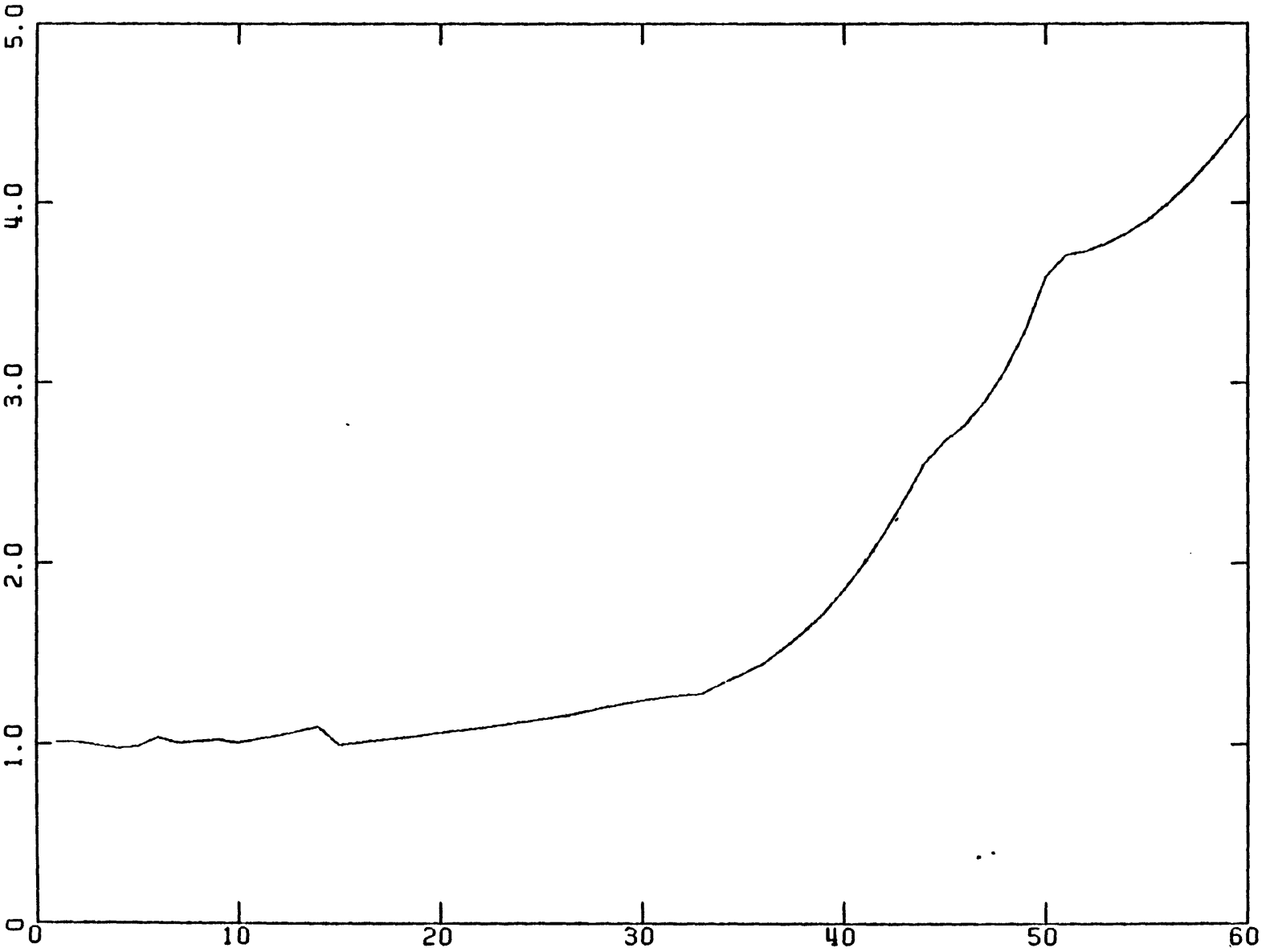
IVDA2-IVDA1, OMEGA 2 = OMEGA 1 DAMPING = .2, CHANNEL 02
RATIO
0
1.0
2.0
3.0
4.0
5.0
0
10
20
30
40
50
60
OMEGA 1

Fig 6

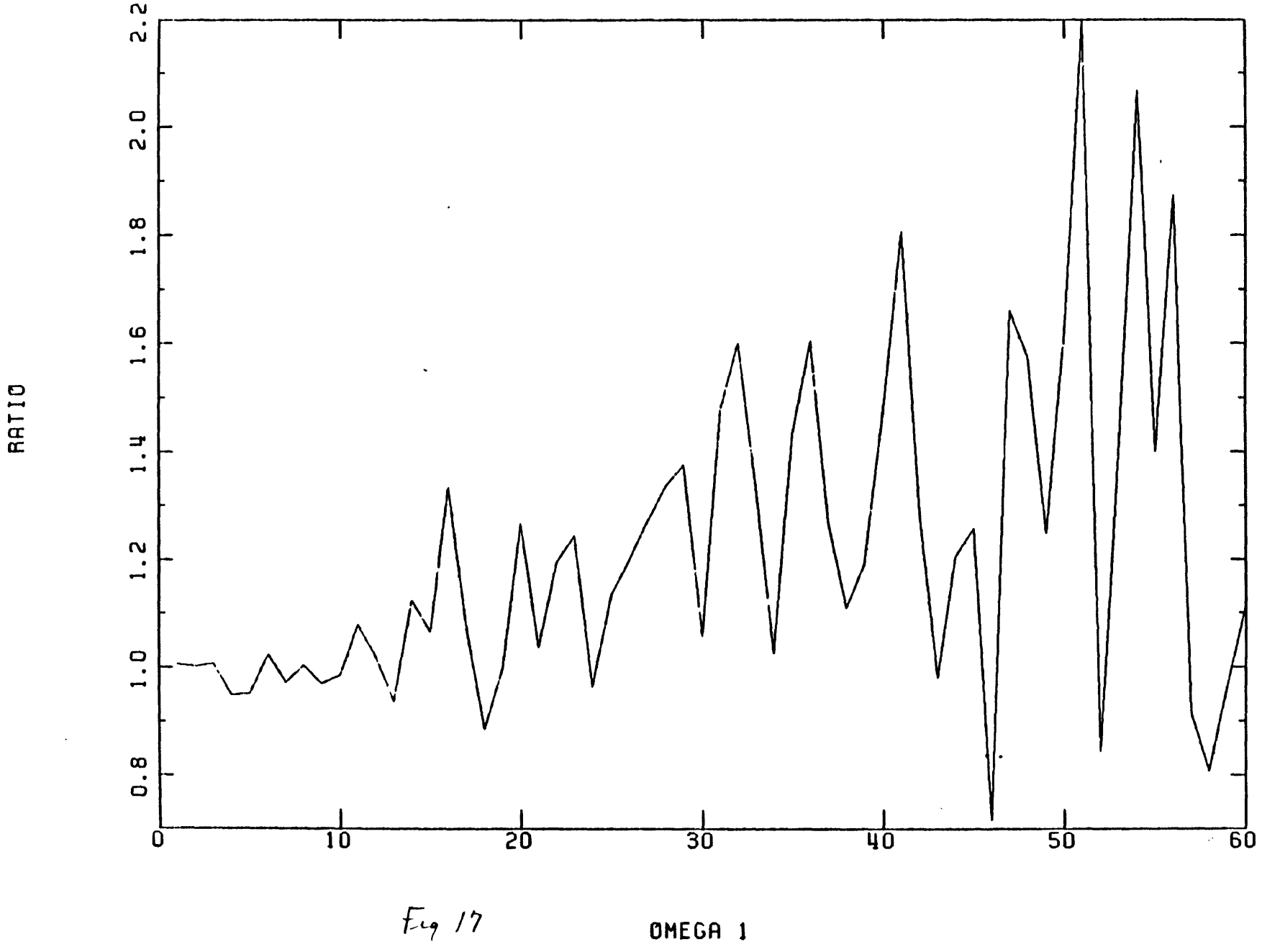
IVDA3-IVDA1, OMEGA 2 = 10.0, CHANNEL 02
RATIO
0.8
1.0
1.2
1.4
1.6
1.8
2.0
2.2
0
10
20
30
40
50
60
OMEGA 1

Fig 17

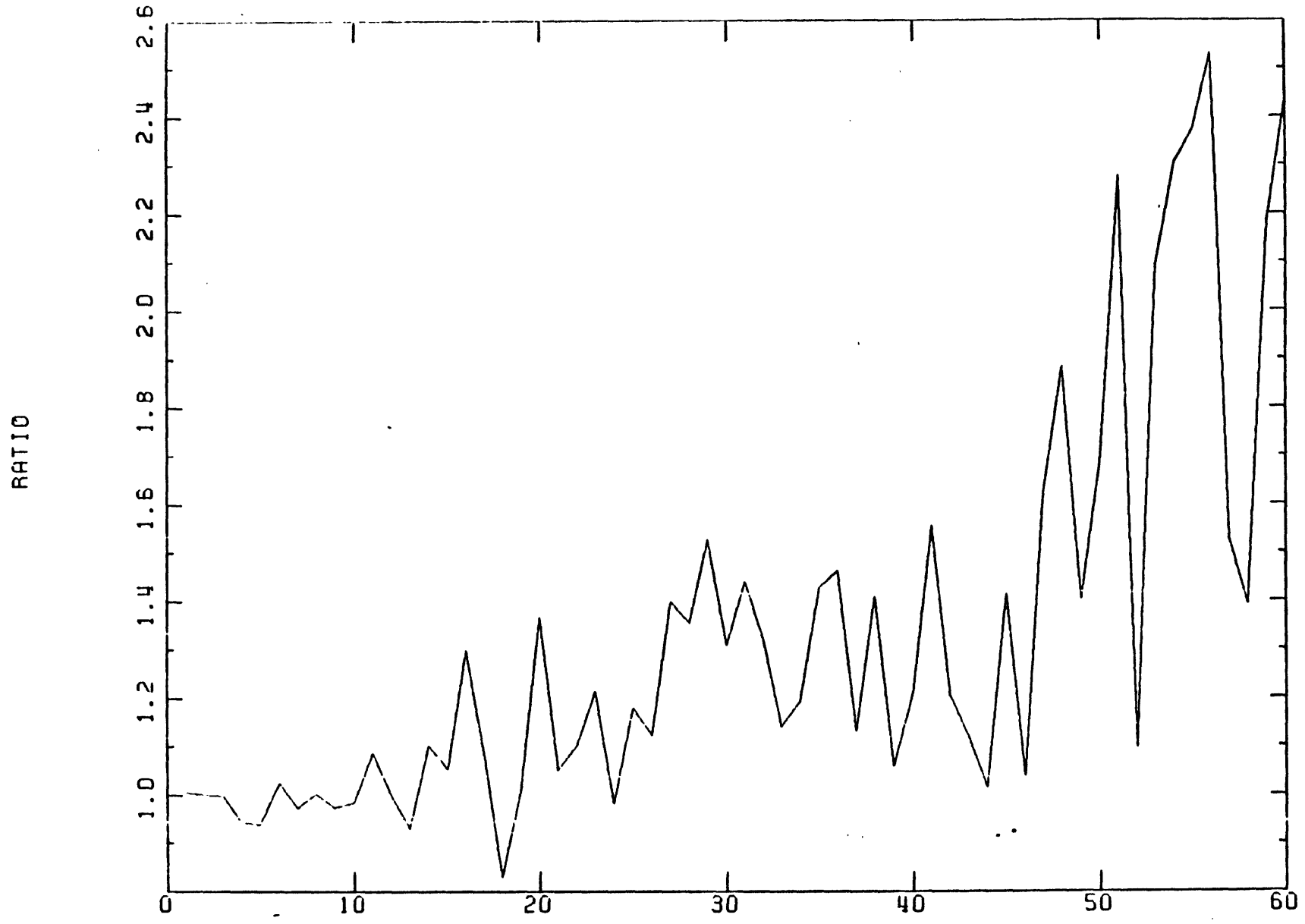
IVDA3 .vDA1 OMEGA 2 = OMEGA 1
RATIO
1.0
1.2
1.4
1.6
1.8
2.0
2.2
2.4
2.6
0
10
20
30
40
50
60
OMEGA 1 AND OMEGA 2

42

Fig 12

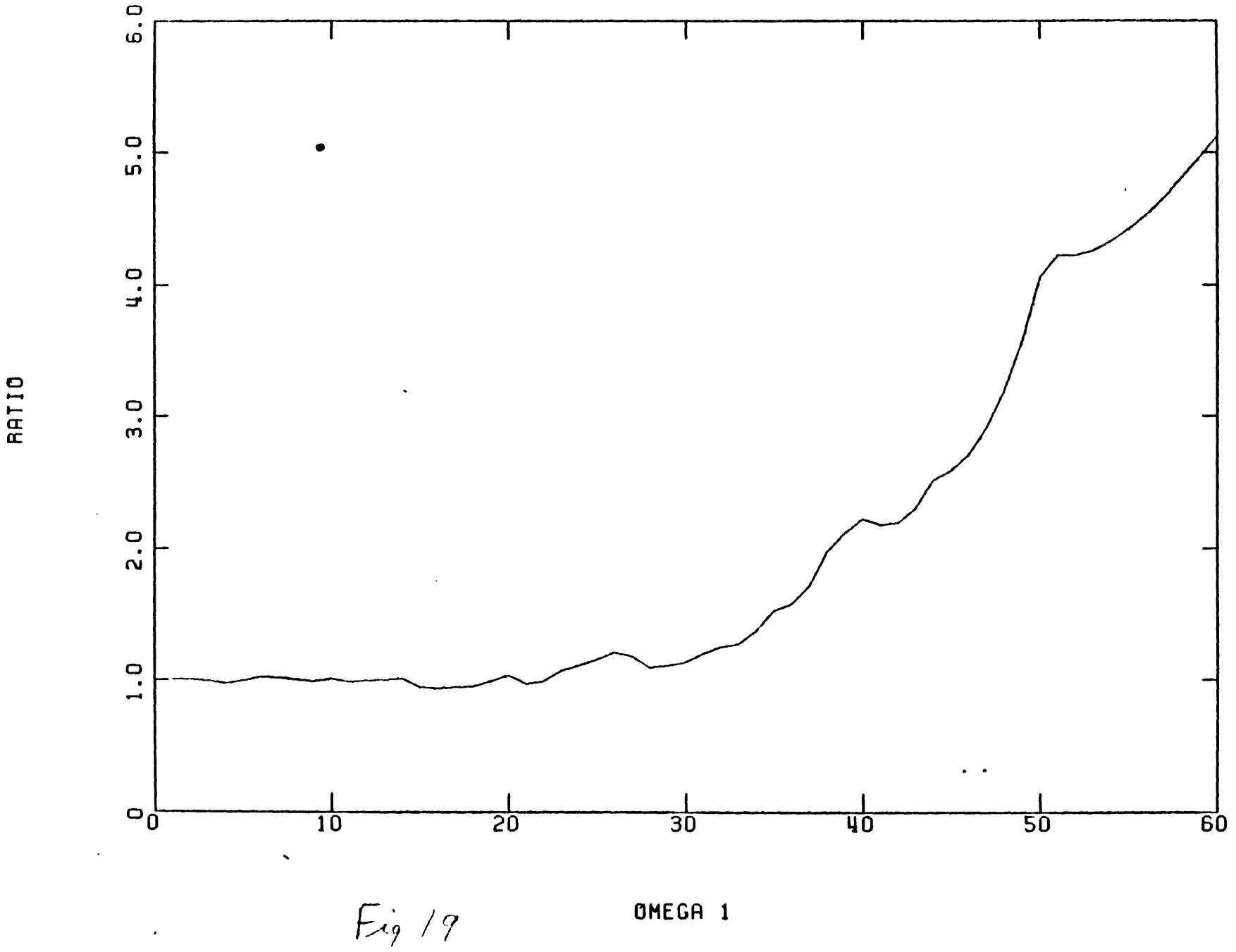
IVDA3-IVDA1, OMEGA 2 = OMEGA 1 DAMPING = .1, CHANNEL 02
RATIO
0
1.0
2.0
3.0
4.0
5.0
6.0
0
10
20
30
40
50
60
OMEGA 1

Fig 19

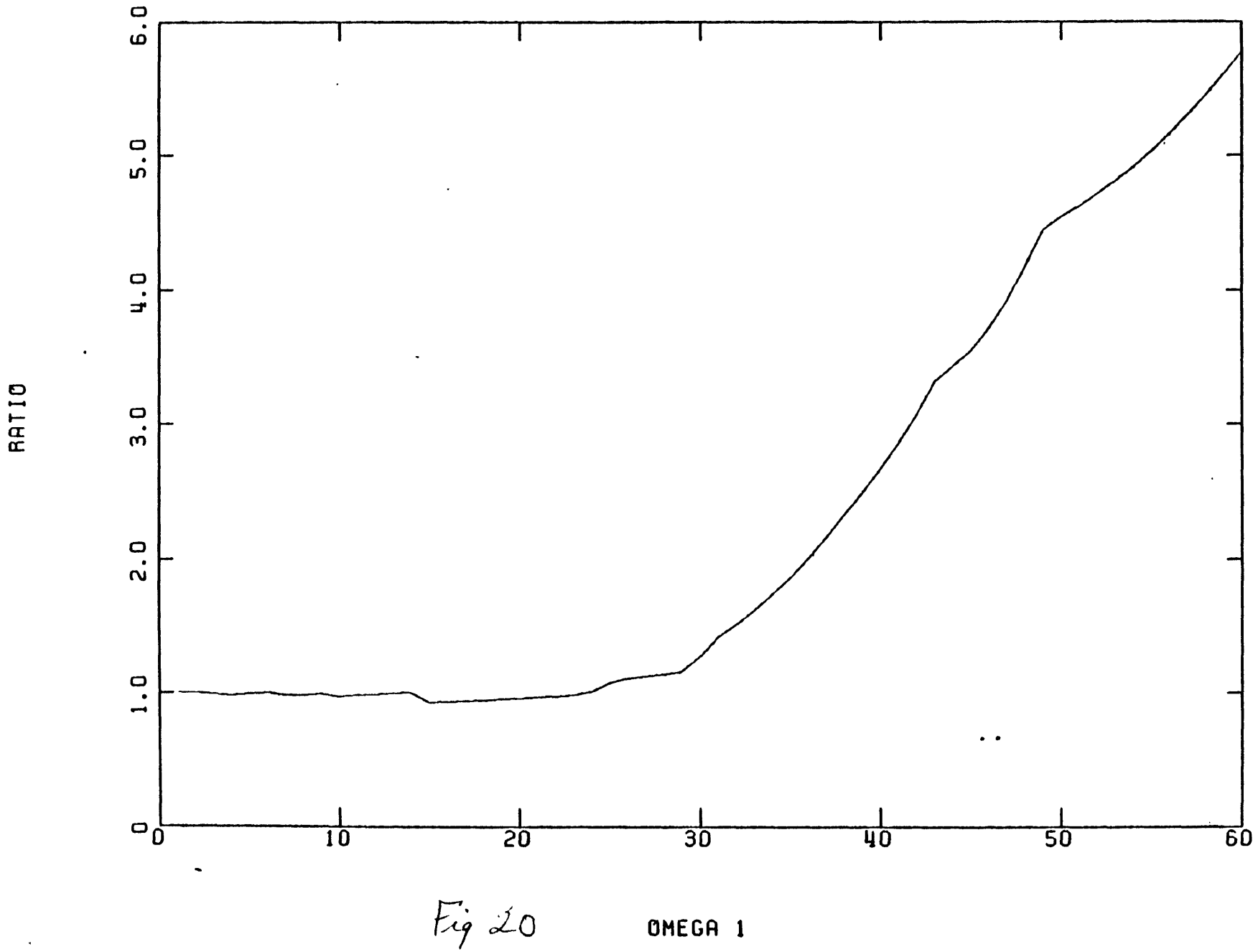
IVDA3-IVDA1, OMEGA 2 = OMEGA 1 DAMPING = .2, CHANNEL 02
RATIO
0
1.0
2.0
3.0
4.0
5.0
6.0
0
10
20
30
40
50
60
OMEGA 1

Fig 20

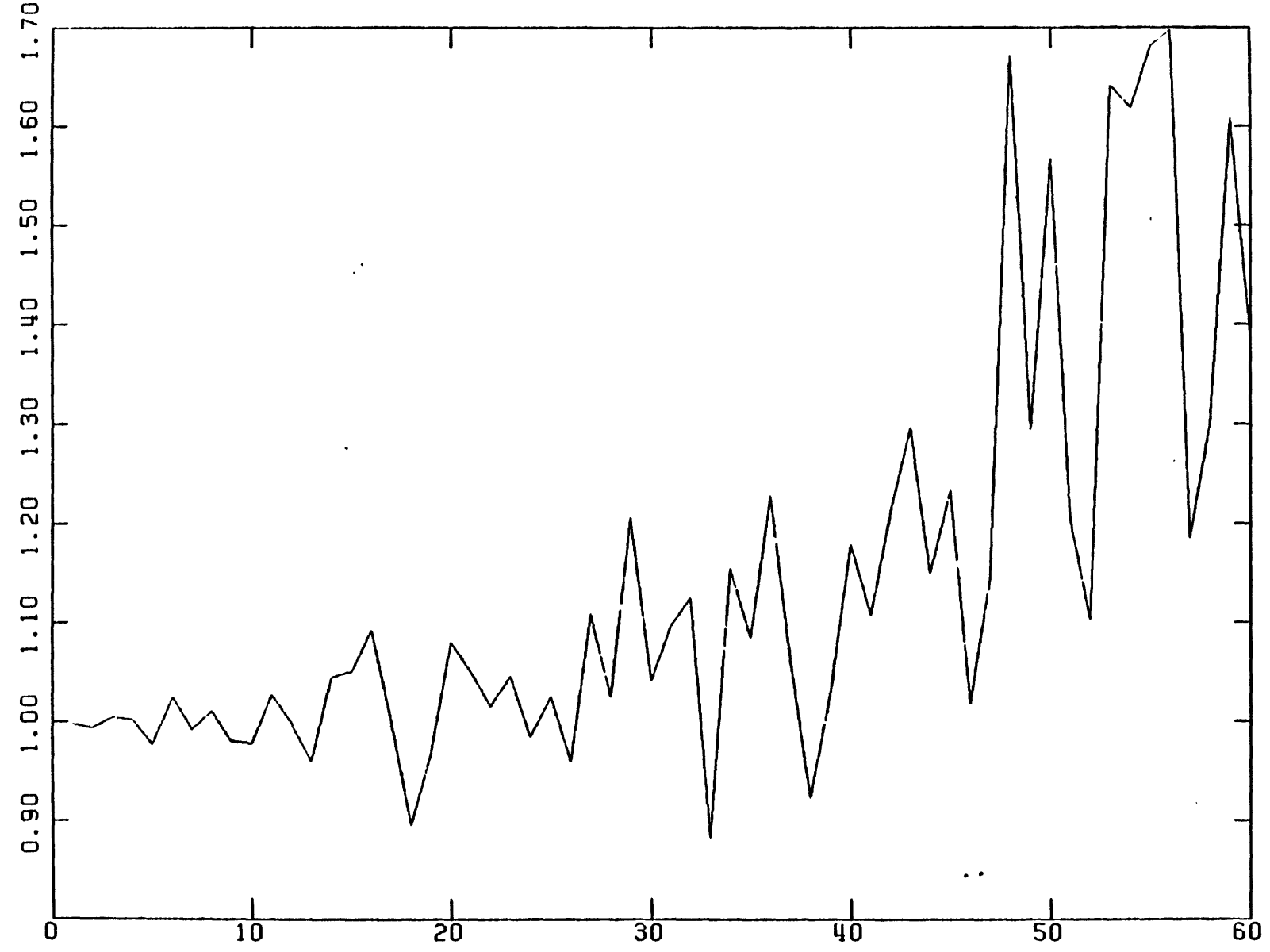
IVDA3-IVDA2, OMEGA 2 = 10.0, CHANNEL 02
RATIO
0.90
1.00
1.10
1.20
1.30
1.40
1.50
1.60
1.70
0
10
20
30
40
50
60
OMEGA 1

Fig 21

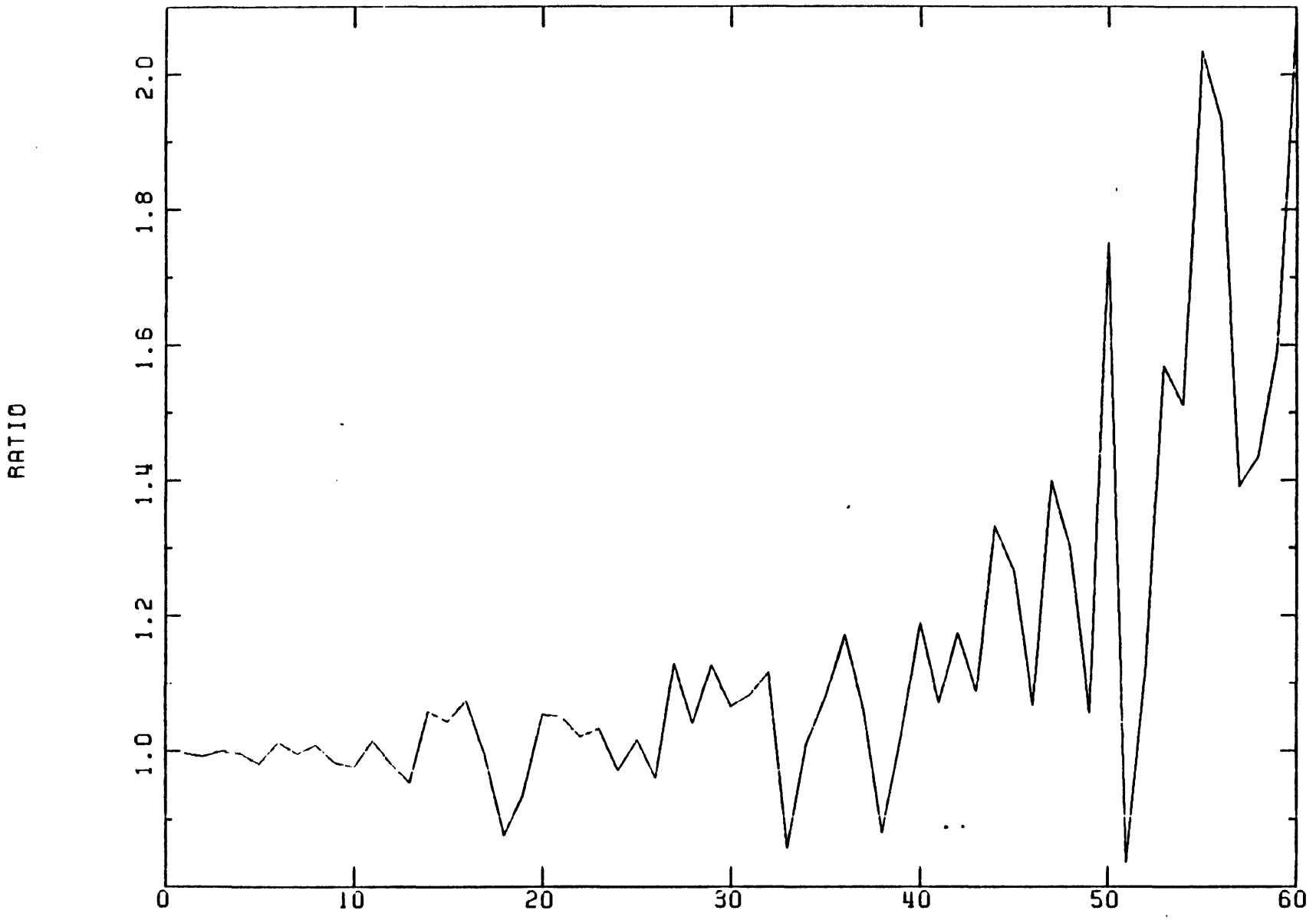
IVDA3 -IVDA2 OMEGA 2 = OMEGA 1
RATIO
1.0
1.2
1.4
1.6
1.8
2.0
0
10
20
30
40
50
60
OMEGA 1 AND OMEGA 2

Fig 22

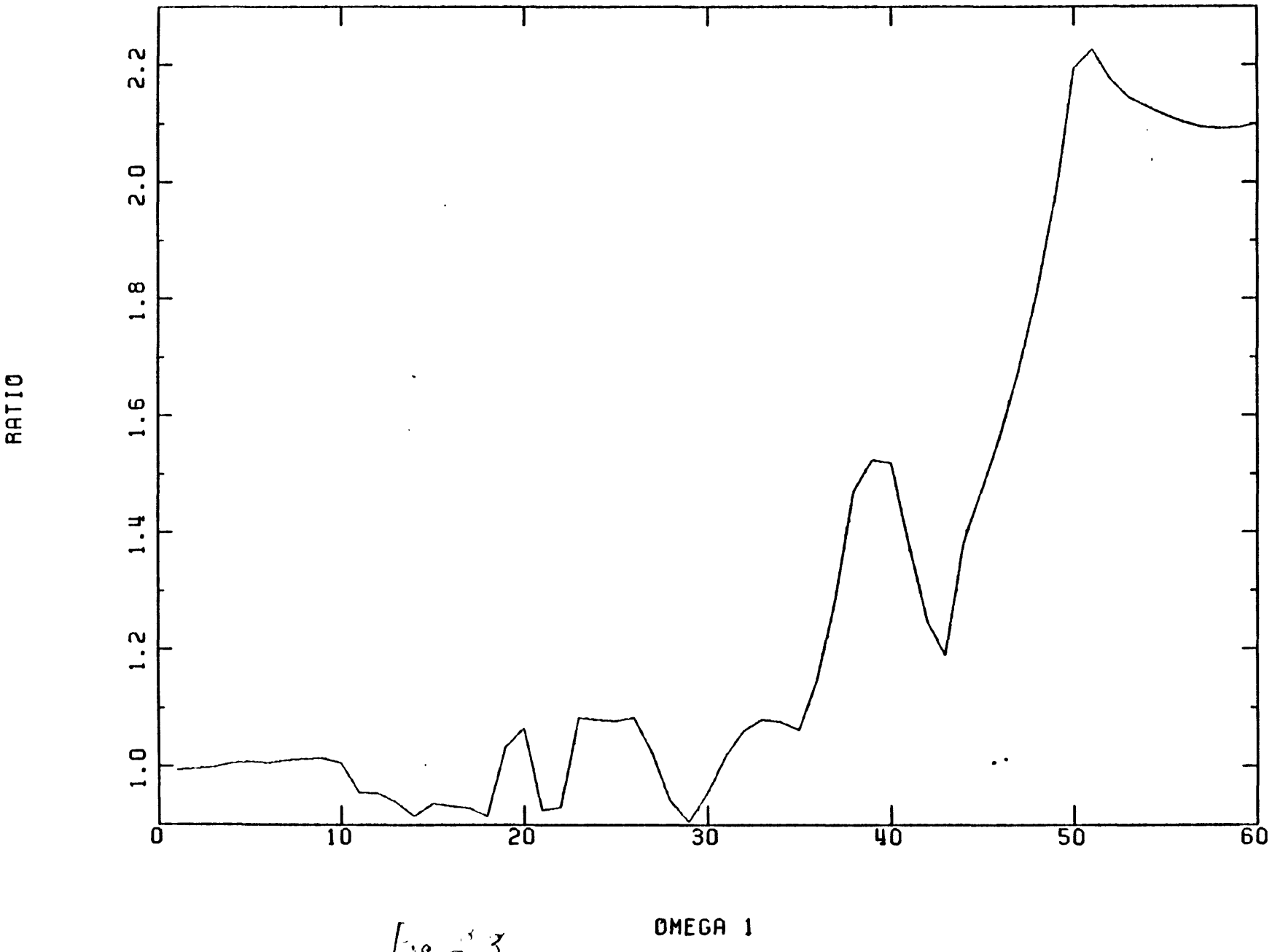
IVDA3-IVDA2, OMEGA 2 = OMEGA 1 DAMPING = .1, CHANNEL 02
RATIO
1.0
1.2
1.4
1.6
1.8
2.0
2.2
0
10
20
30
40
50
60
OMEGA 1

Fig 23

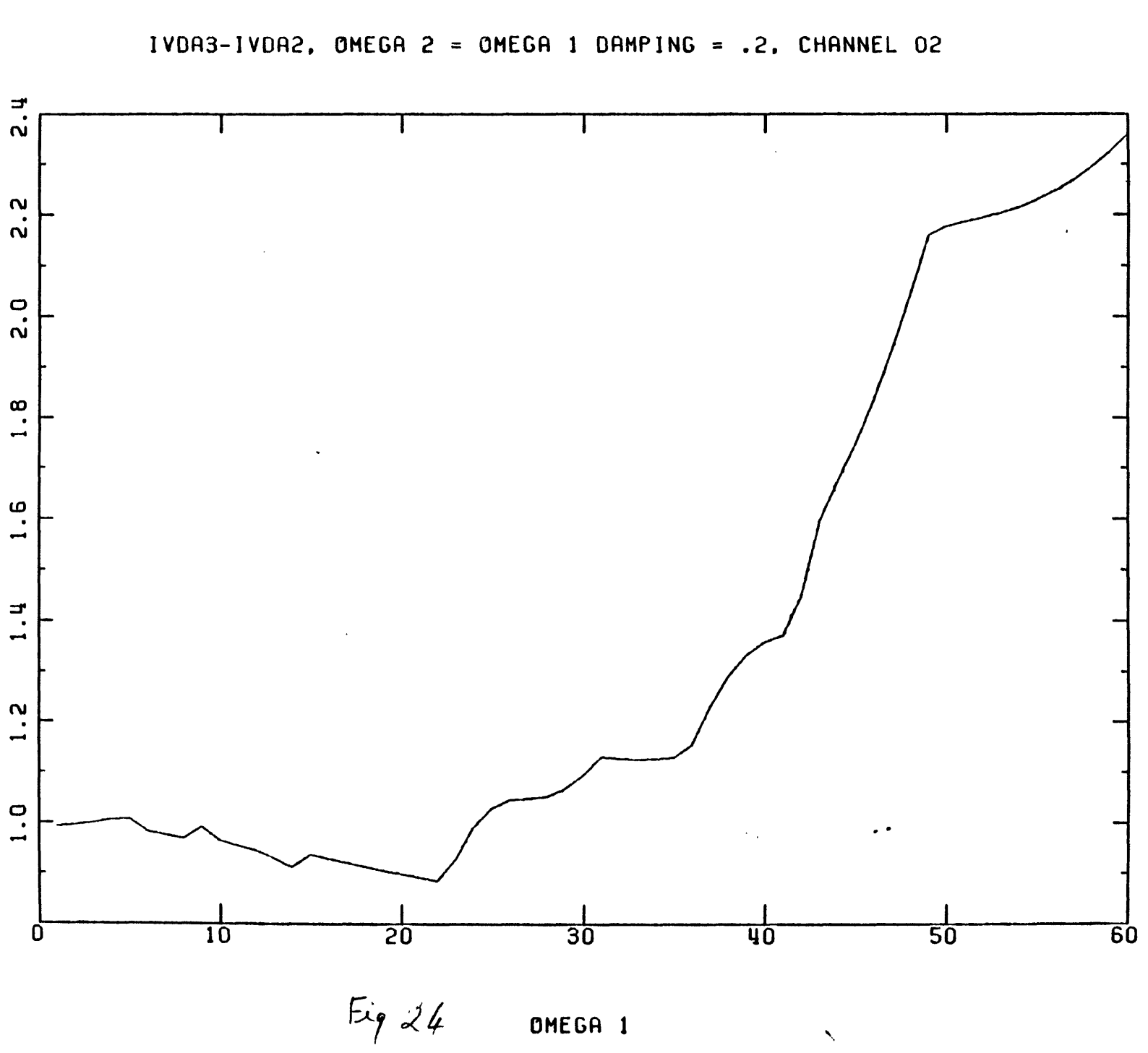
IVDA3-IVDA2, OMEGA 2 = OMEGA 1 DAMPING = .2, CHANNEL 02
RATIO
1.0
1.2
1.4
1.6
1.8
2.0
2.2
2.4
0
10
20
30
40
50
60
OMEGA 1

Fig 24